

## Isoform-Specific Phosphoinositide 3-Kinase Inhibitors Exert Distinct Effects in Solid Tumors

Kyle A. Edgar, Jeffrey J. Wallin, Megan Berry, Leslie B. Lee, Wei Wei Prior, Deepak Sampath, Lori S. Friedman, and Marcia Belvin

### Abstract

Therapeutic inhibitors are being developed against the phosphoinositide 3-kinase (PI3K) pathway, the deregulation of which drives tumor growth and survival in many cancers. There are eight PI3Ks in mammals divided into three classes. Class IA PI3Ks (p110 $\alpha$ , p110 $\beta$ , and p110 $\delta$ ) are critical for cell growth and survival, with the p110 $\alpha$  isoform implicated as the most important in carcinomas. In this study, we examined the effects of small-molecule inhibitors of class IA PI3Ks to explore the contributions of different isoforms in cancer cells. Similar responses were seen in cancer cells with wild-type or activated mutant PI3K genes treated with p110 $\alpha$ / $\delta$  or p110 $\alpha$ / $\beta$ / $\delta$  inhibitors in cell viability assays. In contrast, PTEN-negative cell lines tended to be less responsive (4-fold overall) to an inhibitor of p110 $\alpha$ / $\delta$  versus p110 $\alpha$ / $\beta$ / $\delta$ . Combining a p110 $\alpha$ / $\delta$  inhibitor with a p110 $\beta$  inhibitor resulted in comparable potency to the p110 $\alpha$ / $\beta$ / $\delta$  inhibitor. The disparity in efficacy was confirmed *in vivo*. Pharmacodynamic biomarker analysis revealed that an inhibitor with insufficient potency against the p110 $\beta$  isoform was less effective at inhibiting the PI3K pathway in PTEN-negative tumor xenografts. Our results imply that patients with PTEN-negative tumors may preferentially benefit from treatment with a class I PI3K inhibitor that is capable of inhibiting the p110 $\beta$  isoform. *Cancer Res*; 70(3); 1164–72. ©2010 AACR.

### Introduction

The phosphatidylinositol 3'-kinase (PI3K) signaling pathway can be activated by a variety of extracellular signals and is involved in cellular processes such as survival, proliferation, migration, and protein synthesis. Aberrant activation of this pathway has been widely implicated in many cancers. In recent years, several groups have reported mutations or gene amplifications in the PI3K p110 $\alpha$  catalytic subunit resulting in increased pathway signaling (1–3). The tumor suppressor protein phosphatase and tensin homologue (PTEN) acts to inhibit PI3K pathway signaling and is commonly mutated, deleted, or epigenetically repressed in human cancers (4, 5). In addition, the pathway can be activated by mutations or overexpression of upstream signaling molecules such as epidermal growth factor receptor (EGFR) or ErbB2 (6–8). Due to its involvement in many cancers, there is increasing interest in the development of inhibitors of the PI3K pathway as potential therapeutics.

Catalytic PI3Ks are lipid kinases and can be divided into three different classes (class I, II, and III) according to their structures, substrate preference, tissue distribution, and

mechanism of activation (9–11). Class I PI3Ks are best known in terms of their function in regulating cell proliferation and tumorigenesis. They are composed of a catalytic (p110) and an adaptor subunit (p85/p55/p101). There are three known class IA p110 isoforms (p110 $\alpha$ , p110 $\beta$ , and p110 $\delta$ ) that interact with the adaptor subunits p55 and p85. All class I PI3Ks possess intrinsic protein kinase activity and are recruited to the membrane in a similar manner. Recent studies involving knockout mice involving loss-of-function mutations in p110 knock-in mice, however, have shown functional differences between the isoforms (12, 13). Recent studies have shown that the p110 $\alpha$  and p110 $\delta$  isoforms are downstream of receptor tyrosine kinases (RTK), whereas the two remaining class I isoforms (p110 $\beta$  and p110 $\gamma$ ) are activated through G-protein-coupled receptor (GPCR) signaling (14, 15). The isoforms also possess differential tissue distribution. The p110 $\alpha$  and p110 $\beta$  isoforms are ubiquitously expressed, whereas p110 $\delta$  and p110 $\gamma$  are found predominantly in leukocytes (16).

The most direct approach to inhibiting the PI3K/Akt pathway is to target PI3K itself. Wortmannin and LY294002 both target the catalytic site of all class I p110 isoforms and have been extensively used as research tools (17, 18). Some of the observed effects of these compounds might not be due to inhibition of PI3K because both compounds exhibit a significant amount of off-target activity (17, 19). These inhibitors also have limited use *in vivo* due to toxicities and poor pharmaceutical properties. In recent years, several PI3K inhibitors with more favorable selectivity and *in vivo* properties have entered clinical trials (reviewed in ref. 20). These inhibitors target all class I PI3Ks and some display potency against mammalian target of rapamycin (mTOR).

**Authors' Affiliation:** Cancer Signaling and Translational Oncology, Genentech, Inc., South San Francisco, California

**Note:** Supplementary data for this article are available at Cancer Research Online (<http://cancerres.aacrjournals.org/>).

**Corresponding Author:** Marcia Belvin, Genentech, Inc., 1 DNA Way, South San Francisco, CA 94080. Phone: 650-467-7346; Fax: 650-225-1411; E-mail: mbelvin@gene.com.

doi: 10.1158/0008-5472.CAN-09-2525

©2010 American Association for Cancer Research.

One challenge to pharmacologic targeting of the PI3K family is to define the individual contributions of each class I isoform to the functions of normal and cancer cells. The use of isoform-specific compounds would significantly facilitate defining the roles of each isoform, and selective small-molecule inhibitors for p110 $\beta$  (TGX-221) and p110 $\delta$  have already been made (21, 22). It will be particularly important to understand the contributions of p110 $\alpha$  and p110 $\beta$  in solid tumors based on their abundant expression in these tumors. Due to the involvement of the PI3K pathway in insulin signaling, normal cell toxicities with p110 isoform inhibition must also be considered. Recent genetic studies have indicated that inhibition of p110 $\alpha$  can have effects on insulin signaling and glucose metabolism (12). Clearly, an understanding of the balance between efficacy and toxicities will be necessary.

In these studies, we investigated the effect of PI3K isoform-selective inhibitors on viability and signaling in solid tumor cell lines. We found that inhibition of the p110 $\alpha$  and p110 $\delta$  isoforms was sufficient to impede growth to the same extent as with inhibition of all three class IA p110 isoforms in lines that contained functional PTEN protein. In cell lines lacking the tumor suppressor PTEN, however, we found that inhibition of all three class IA p110 isoforms resulted in significantly improved efficacy. These results were reproduced *in vivo* when we compared a PI3K inhibitor with potency against all isoforms to a similar inhibitor that lacks potency against p110 $\beta$ , and observed differential efficacy in a PTEN-negative xenograft model.

## Materials and Methods

**Cell culture.** Cell lines were cultured in DMEM or RPMI supplemented with 10% fetal bovine serum, 100 units/mL penicillin, and 100  $\mu$ g/mL streptomycin at 37°C under 5% CO<sub>2</sub>. MCF7.1 is an *in vivo* selected cell line developed at Genentech, Inc., and derived from the parental MCF7 human breast cancer cell line (American Type Culture Collection).

**Compounds and reagents.** GDC-0941 and PI3Ki-A/D were obtained from Genentech. TGX-221 was obtained from Calbiochem.

**Cell viability assays.** Cells were seeded (1,000–2,000 per well) in 384-well plates for 16 h. On day 2, nine serial 1:2 compound dilutions were made in DMSO in a 96-well plate. The compounds were then further diluted into growth media using a Rapidplate robot (Zymark Corp.). The diluted compounds were then added to quadruplicate wells in the 384-well cell plates and incubated at 37°C and 5% CO<sub>2</sub>. After 4 d, relative numbers of viable cells were measured by luminescence using Cell Titer-Glo (Promega) according to the manufacturer's instructions and read on a Wallac Multilabel Reader (Perkin-Elmer). EC<sub>50</sub> values were calculated using Prism 4.0 software (GraphPad).

**Cell cycle analysis.** Cells were treated with GDC-0941 or PI3Ki-A/D at the indicated concentrations for 48 h, then harvested with 0.25% trypsin and washed with PBS. Cells at a density of 1  $\times$  10<sup>6</sup>/mL were fixed in 100% ice-cold ethanol and stored at –20°C overnight, then washed with PBS and incubated in propidium iodide (PI) solution [0.1% Triton-X,

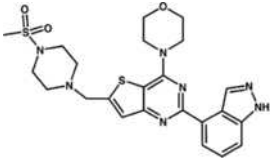
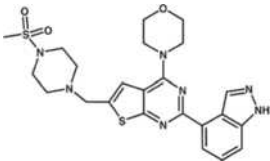
0.2 mg/mL RNase solution (Sigma), 0.05 mg/mL PI solution (Sigma), in PBS] for 30 min at room temperature in the dark. Cells were immediately analyzed with a FACScan flow cytometer (Becton Dickinson).

**In vitro pharmacodynamic assays.** Levels of pAkt (Ser<sup>473</sup>) and pPras40 (Thr<sup>246</sup>) were assessed using bead kits from Biosource and the Luminex Bio-Plex system measuring fluorescence intensity (Bio-Rad). Levels of pS6 (Ser<sup>235/236</sup>) were determined using an ELISA measuring absorbance at 450 nm (Cell Signaling Technology). For Western blots, equal amounts of protein were separated by electrophoresis through NuPage Bis-Tris 4–12% gradient gels (Invitrogen); proteins were transferred onto nitrocellulose pore membranes using the iBlot system and protocol from Invitrogen. pAkt (Ser<sup>473</sup>) antibody was obtained from Cell Signaling Technology. The PTEN antibody was obtained from BD Pharmingen. Specific antigen-antibody interaction was detected with a horseradish peroxidase-conjugated secondary antibody IgG using enhanced chemiluminescence Western blotting detection reagents (Amersham Biosciences).

**In vivo xenograft studies.** Human prostate cancer PC3-NCI cells obtained from the National Cancer Institute (Frederick, MD) were resuspended in HBSS and implanted s.c. into the right hind flanks of nude mice. Tumors were monitored until they reached a mean tumor volume of 150 to 200 mm<sup>3</sup> before the initiation of dosing. MCF7.1 cells resuspended in a 1:1 mixture of HBSS and Matrigel Basement Membrane Matrix (BD Biosciences) were s.c. implanted into the right hind flank of each mouse. Before cell inoculation, 17 $\beta$ -estradiol (0.36 mg/pellet, 60-d release), obtained from Innovative Research of America, were implanted into the dorsal shoulder blade areas of nude mice. After implantation of cells into mice, tumors were monitored until they reached a mean tumor volume of 250 to 350 mm<sup>3</sup> before initiating dosing. GDC-0941 and PI3Ki-A/D were obtained as solutions and dissolved in 0.5% methylcellulose with 0.2% Tween-80 (MCT). Female nude (nu/nu) mice that were 6 to 8 wk old and weighed 20 to 30 g were obtained from Charles River Laboratories. Tumor-bearing mice were dosed daily for 14 to 21 d, depending on the xenograft model, with 100  $\mu$ L of vehicle (MCT), 75 mg/kg GDC-0941, or 75 mg/kg PI3Ki-A/D orally.

Tumor volume was measured in two dimensions (length and width) using Ultra Cal-IV calipers (model 54-10-111, Fred V. Fowler Company) and was analyzed using Excel version 11.2 (Microsoft Corporation). Tumor volume (mm<sup>3</sup>) = (longer measurement  $\times$  shorter measurement<sup>2</sup>)  $\times$  0.5. Animal body weights were measured using an Adventurer Pro AV812 scale (Ohaus Corporation). Percent weight change = [1 – (new weight/initial weight)]  $\times$  100. Tumor sizes were recorded twice weekly over the course of the study (14–21 d). Mouse body weights were also recorded twice weekly and the mice were observed daily. Mice with tumor volumes  $\geq$ 2,000 mm<sup>3</sup> or with losses in body weight  $\geq$ 20% from their initial body weight were promptly euthanized per Institutional Animal Care and Use Committee guidelines. Mean tumor volume and SEM values ( $n$  = 10) were calculated using JMP statistical software, version 5.1.2, at the end of treatment. Percent tumor inhibition = 100  $\times$  [(mean volume of

**Table 1.** Compound characterization for GDC-0941 and PI3Ki-A/D

Compound ID		p110 $\alpha$ IC <sub>50</sub> ( $\mu$ mol/L)	p110 $\beta$ IC <sub>50</sub> ( $\mu$ mol/L)	p110 $\delta$ IC <sub>50</sub> ( $\mu$ mol/L)	p110 $\gamma$ IC <sub>50</sub> ( $\mu$ mol/L)	DNA-PK IC <sub>50</sub> ( $\mu$ mol/L)	mTOR K <sub>i</sub> ( $\mu$ mol/L)
GDC-0941		0.003	0.033	0.003	0.075	1.23	0.580
PI3Ki-A/D		0.003	0.332	0.010	0.112	0.743	1.200

NOTE: Biochemical IC<sub>50</sub> values for the PI3K isoforms (p110 $\alpha$ , p110 $\beta$ , p110 $\delta$ , and p110 $\gamma$ ), DNA-PK, and mTOR for GDC-0941 and PI3Ki-A/D.

tumors in vehicle treated animals – mean volume of tumors in test article treated animals given the test article)/mean volume of tumors in vehicle treated animals]. Data were analyzed and *P* values were determined using Student's *t* test with JMP statistical software, version 5.1.2 (SAS Institute).

For pharmacodynamic analysis of the PI3K/Akt pathway *in vivo*, NCI-PC3 or MCF7.1 tumors were excised from animals and immediately snap frozen in liquid nitrogen. Frozen tumors were weighed and lysed with a pestle PP (Scienceware) in cell extract buffer (Biosource) supplemented with protease inhibitors (F. Hoffman-LaRoche Ltd.), 1 mmol/L phenylmethanesulfonyl fluoride, and phosphatase inhibitor cocktails 1 and 2 (Sigma). Protein concentrations were determined using the Pierce BCA Protein Assay Kit. Levels of pAkt (Ser<sup>473</sup>) and pS6 (Ser<sup>235/236</sup>) were assessed using kits measuring luminescence (Meso Scale Discovery). Levels of pPras40 (Thr<sup>246</sup>) were determined using an ELISA measuring absorbance at 450 nm (Biosource). Data were analyzed and *P* values were determined using Student's *t* test with JMP statistical software, version 5.1.2 (SAS Institute). Tumor drug concentrations were also measured from frozen samples by a liquid chromatography-tandem mass spectrometry assay in the Drug Metabolism and Pharmacokinetic Bioanalytical Department at Genentech, and the lower limit of quantitation for detectable levels was 0.005  $\mu$ mol/L.

## Results

We used a pair of PI3K inhibitors (Table 1) with different selectivity profiles than the p110 subunits of PI3K to investigate their therapeutic potential in solid tumors. GDC-0941 is a pan inhibitor of PI3K with IC<sub>50</sub> values in the low nanomolar range for all three of the class IA p110 isoforms (23). PI3Ki-A/D is a selective inhibitor of the p110 $\alpha$  and p110 $\delta$  isoforms,

sparing p110 $\beta$  inhibition more than 100-fold relative to the inhibition of p110 $\alpha$  (24). Neither molecule significantly inhibits mTOR or DNA-dependent protein kinase (DNA-PK; Table 1), and both display excellent selectivity over a panel of 228 kinases in the KinaseProfiler panel from Millipore (ref. 23 and data not shown).

To assess the *in vitro* effects of GDC-0941 and PI3Ki-A/D, we investigated a panel of 102 solid tumor cell lines, consisting of breast, colon, glioma, non-small cell lung, melanoma, ovarian, and prostate cancer cell lines, in a cell viability assay. The two inhibitors were tested to obtain half maximal effective concentration (EC<sub>50</sub>) values to detect any significant difference in the sensitivity of the two inhibitors as single agents (Supplementary Tables S1–S7). To identify molecular markers that correlate with differential sensitivity between the two compounds, we evaluated the genotypes and protein expression levels of a set of genes in relevant signaling pathways in all of the cell lines. The only significant predictor of sensitivity observed was PTEN status as assessed by the presence or absence of PTEN protein by immunoblotting, as well as the presence of inactivating mutations in the PTEN sequence. There was no observed change in relative sensitivity dependent on p110 $\alpha$  activating mutational status (Fig. 1B). The lines that were negative for PTEN showed higher sensitivity to GDC-0941 than they did to PI3Ki-A/D, with GDC-0941 being on average 3.97-fold more potent (Fig. 1B). PTEN-positive lines showed very similar sensitivity between the two inhibitors, with an average difference of 1.59-fold. When lines were grouped by PIK3CA and PTEN status, the fold difference in sensitivity was statistically significant (*P* < 0.0001) between PIK3CA wild-type and PTEN-negative lines as well as between PIK3CA-mutant and PTEN-negative lines (Fig. 1B). This difference was observed across all tumor types (Supplementary Fig. S1).

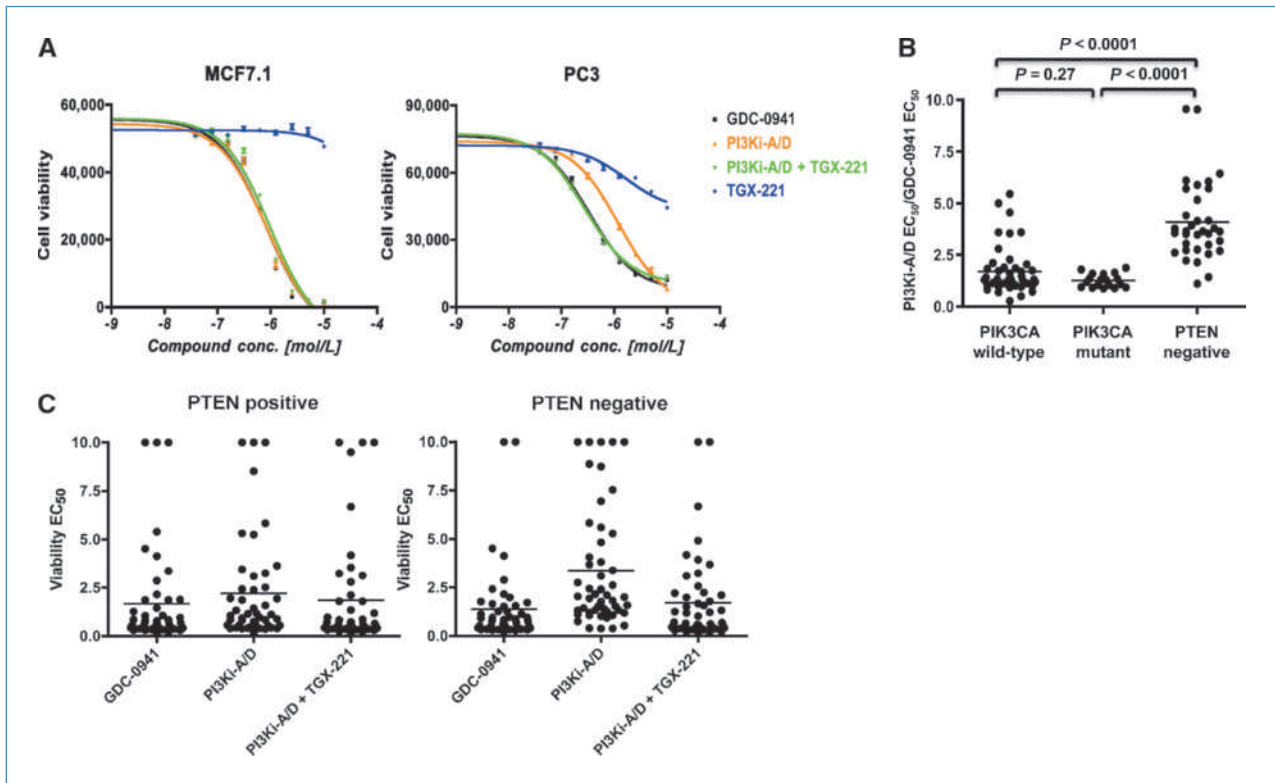


**Figure 1.** Cell viability effects of GDC-0941 and PI3Ki-A/D in a panel of solid tumor cell lines. A, two cell lines, MCF7.1 (PTEN positive) and PC3 (PTEN negative), were treated with GDC-0941, PI3Ki-A/D, TGX-221, or the combination of PI3Ki-A/D and TGX-221, and assayed for viability using Cell Titer-Glo. B, fold increase in viability EC<sub>50</sub> values for PI3Ki-A/D relative to GDC-0941 in a full panel of 99 solid tumor lines binned by PIK3CA mutational status and PTEN status (the three dual PIK3CA-mutant and PTEN-negative lines were excluded for this analysis). *P* values were determined by Student's *t* test. C, comparison of viability EC<sub>50</sub> values (μmol/L) of solid tumor lines when separated into PTEN-positive and PTEN-negative cell lines and dosed with GDC-0941, PI3Ki-A/D, or the combination of PI3Ki-A/D and TGX-221.

To confirm that the difference in sensitivity between GDC-0941 and PI3Ki-A/D was due to their different p110 selectivity profiles, we used a specific p110β inhibitor, TGX-221 (21). In the PTEN-negative prostate line PC3, which was 3.5-fold more sensitive to GDC-0941 than to PI3Ki-A/D, the addition of TGX-221 to PI3Ki-A/D increases its potency to that of GDC-0941 (Fig. 1A). In the PTEN-positive cell line MCF7.1, which was equipotent for the two compounds, no increase in sensitivity was observed with the addition of TGX-221 to PI3Ki-A/D. The benefit of inhibiting p110β in PTEN-negative cell lines and the lack of benefit in PTEN-positive lines were observed across a panel of cell lines and across all tumor types (Fig. 1C). We also found that TGX-221 has no observed effect on cell viability as a single agent in PTEN-positive cells, whereas in the majority of PTEN-negative cell lines tested, it showed a cell growth inhibitory effect of up to 40%, yet not enough inhibition to generate an EC<sub>50</sub> value (data not shown).

To further investigate the effects of selective p110 isoform inhibition, we explored the effects of the different compounds on RTK and GPCR stimulation. Recent studies have implicated p110α as a mediator of RTK signaling and p110β as a mediator of GPCR signaling (14, 15). We used epidermal growth factor (EGF) to stimulate the EGFR

and lysophosphatidic acid (LPA) to stimulate GPCR signaling and monitored receptor activation by the increase in pAkt. Both EGF and LPA were capable of inducing pAkt (Fig. 2). GDC-0941, when dosed at its viability EC<sub>50</sub> of

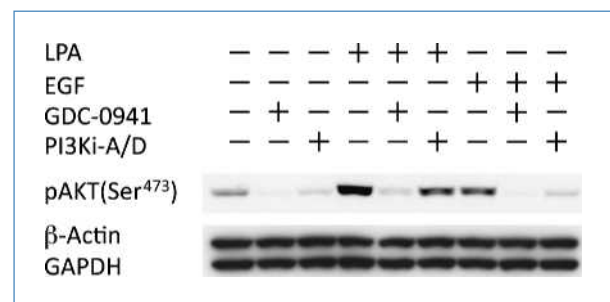


**Figure 2.** Downstream effects of p110 isoform inhibition. PC3 (PTEN-negative) cells were serum starved overnight and simultaneously treated with GDC-0941 or PI3Ki-A/D at their cell viability assay EC<sub>50</sub> (0.34 and 1.2 μmol/L, respectively) and stimulated with either EGF (0.1 μg/mL) or LPA (11.5 μg/mL). After 1 h, cell lysates were prepared and analyzed by immunoblotting for pAkt (Ser<sup>473</sup>) (upper band) or β-actin and GAPDH (two lower bands, respectively) for loading controls.

0.34  $\mu\text{mol/L}$ , was able to inhibit stimulation by either LPA or EGF, whereas PI3Ki-A/D, when dosed at its viability  $\text{EC}_{50}$  of 1.2  $\mu\text{mol/L}$ , was able to block EGF stimulation to a much greater extent than LPA stimulation. Although there was some inhibition of LPA stimulation by PI3Ki-A/D, it was

minimal when compared with the inhibition by GDC-0941 dosed at a 3.5-fold lower dose.

We further investigated the role of inhibiting the class IA p110 isoforms by examining downstream PI3K pathway markers. We dosed all compounds at the  $\text{EC}_{50}$  doses of the

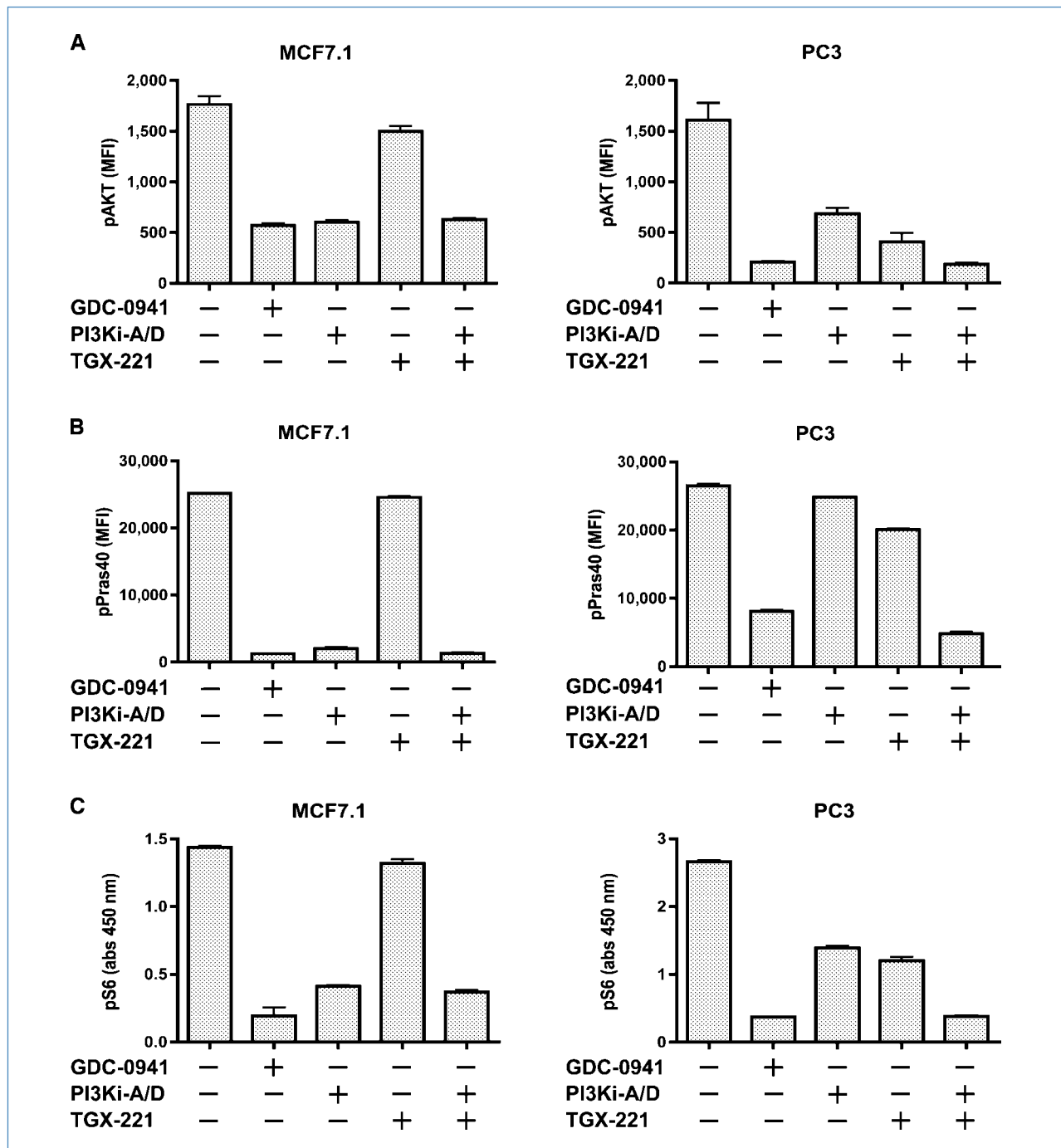
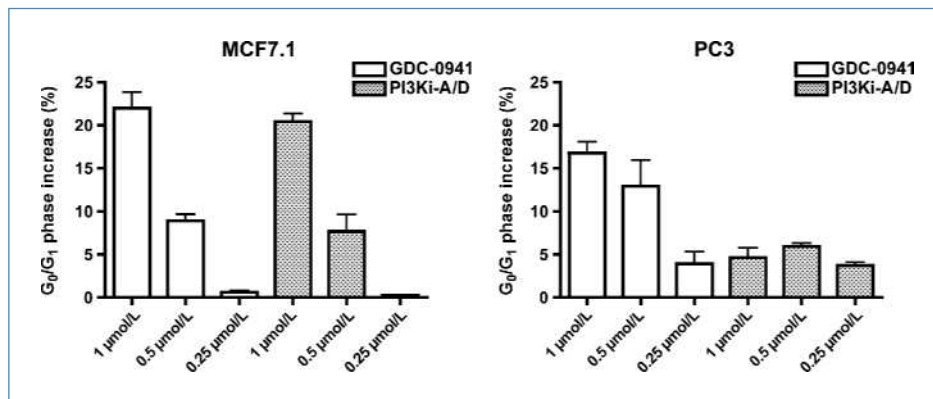


**Figure 3.** *In vitro* pathway effects of GDC-0941 and PI3Ki-A/D. A, cell lines were treated with GDC-0941, PI3Ki-A/D, TGX-221, or the combination of PI3Ki-A/D and TGX-221 at the  $\text{EC}_{50}$  value of GDC-0941 (0.81  $\mu\text{mol/L}$  for MCF7.1 and 0.34  $\mu\text{mol/L}$  for PC3). After 4 h, cell lysates were prepared and analyzed by Luminex assay for pAkt (Ser<sup>473</sup>). B, lysates were analyzed by Luminex assay for pPras40 (Thr<sup>246</sup>). C, lysates were analyzed by ELISA for pS6 (Ser<sup>235/236</sup>). abs, absorbance.

**Figure 4.** Cell cycle effects of GDC-0941 and PI3Ki-A/D. Two cell lines, MCF7.1 (PTEN positive) and PC3 (PTEN negative), were treated with GDC-0941 or PI3Ki-A/D at three doses: 1, 0.5, and 0.25  $\mu\text{mol/L}$ . The cells were treated for 48 h and analyzed by PI/FACS to assess the effects on cell cycle. The percentage of cells in the  $G_1$  stage of the cell cycle was quantified and plotted.



pan-PI3K inhibitor GDC-0941 (0.81  $\mu\text{mol/L}$  for MCF7.1 and 0.34  $\mu\text{mol/L}$  for PC3), so that any difference in pathway marker levels from PI3Ki-A/D could be attributed to the lack of inhibition of the p110 $\beta$  isoform. In MCF7.1 cells (PTEN positive), GDC-0941 and PI3Ki-A/D both significantly reduced pAkt, pPras40, and pS6 levels at 4 hours after treatment, whereas TGX-221 did not have a significant effect on any of the markers (Fig. 3A–C). Furthermore, the addition of TGX-221 to PI3Ki-A/D did not reduce the levels of any of the markers to a greater extent than did PI3Ki-A/D as a single agent. In contrast, in PC3 cells, GDC-0941 strongly reduced all three of the markers, whereas both PI3Ki-A/D and TGX-221 had a significantly weaker effect (Fig. 3A–C). Unlike MCF7.1 cells, PC3 cells showed reduction equal to that with GDC-0941 of all three pathway markers with the combination of PI3Ki-A/D and TGX-221 (Fig. 3A–C).

To investigate the downstream effects of inhibiting all three p110 isoforms versus p110 $\alpha$  and p110 $\delta$  only, cell lines were treated with three doses (1.0, 0.5, and 0.25  $\mu\text{mol/L}$ ) of either GDC-0941 or PI3Ki-A/D, stained with propidium iodide (PI), and analyzed by fluorescent activated cell sorting (FACS) analysis at 48 hours after treatment (Fig. 4). The two compounds increased the  $G_1$  fractions equally in a dose-dependent manner in the PTEN-positive cell line MCF7.1. However, in PC3, the higher doses of GDC-0941 caused an increase in the  $G_1$  fraction, whereas PI3Ki-A/D did so only minimally.

To confirm our *in vitro* findings *in vivo*, we compared GDC-0941 and PI3Ki-A/D in PTEN-positive and PTEN-negative xenograft models. In MCF7.1 breast tumor xenografts (PTEN positive), PI3Ki-A/D and GDC-0941 were equipotent and statistically caused significant tumor inhibition ( $P < 0.0001$ ) compared with vehicle control-treated animals, when dosed daily at 75 mg/kg (Fig. 5A). Alternatively, in NCI-PC3 prostate tumor xenograft models (PTEN negative), PI3Ki-A/D was less potent and did not cause significant tumor inhibition ( $P = 0.19$ ) compared with vehicle control-treated animals, whereas GDC-0941 resulted in significant tumor inhibition when compared with vehicle control ( $P = 0.01$ ; Fig. 5A). Additionally, the antitumor response between GDC-0941 and PI3Ki-A/D was significantly different ( $P = 0.04$ ) in the NCI-PC3 model. The doses tested for PI3Ki-A/D and GDC-0941 were well tolerated because body weights were comparable between the vehicle and treated animals (Supplementary

Fig. S2) and produced similar drug tumor levels (Supplementary Table S8A and B).

The differences in efficacy between GDC-0941 and PI3Ki-A/D in xenograft models correlated with the effect of each drug on PI3K/Akt pathway suppression *in vivo*. GDC-0941 and PI3Ki-A/D suppressed pAkt, pPras40, and pS6 equivalently 4 hours after a single dose in PTEN-positive MCF7.1 tumors (Fig. 5B–D). Conversely, the effects on pAkt, pPras40, and pS6 suppression were significantly less pronounced at 4 hours after a single dose of PI3Ki-A/D compared with an equivalent dose of GDC-0941 in PTEN-negative NCI-PC3 tumors (Fig. 5B–D).

## Discussion

Establishing the roles of p110 $\alpha$  and p110 $\beta$  isoforms in cancer cell signaling has been complicated by the lack of specific high-quality isoform-selective inhibitors. Here, we describe the characterization of two potent and selective PI3K inhibitors *in vitro* and *in vivo*. GDC-0941 inhibits all class IA isoforms, whereas PI3Ki-A/D selectively blocks the activity of p110 $\alpha$  and p110 $\delta$ . Neither compound potently inhibits DNA-PK, TORC1, or TORC2, and both are selective for PI3K against a large panel of other kinases. The compounds also have similar pharmacokinetic properties in terms of clearance, volume of distribution, and bioavailability (ref. 23; Table 2). Use of these two inhibitors has allowed us to investigate the effects of specific PI3K class IA isoform inhibition.

GDC-0941 and PI3Ki-A/D were tested in a large panel of cancer cell lines to evaluate their cellular potency. In the majority of cell lines, the two inhibitors were equipotent in the Cell Titer-Glo assay. In PTEN-negative lines, however, GDC-0941 exhibited approximately 4-fold greater potency. Use of the p110 $\beta$  inhibitor confirmed that the disparity between PTEN-negative and PTEN-positive lines was due to an increased reliance on the p110 $\beta$  isoform. The potency differences of the inhibitors were also shown in the effects on downstream biomarkers in the PI3K pathway. Although there was increased efficacy with GDC-0941 over PI3Ki-A/D in PTEN-negative lines, the two inhibitors were not significantly different in cell lines harboring activating mutations in PIK3CA. Not only did PIK3CA mutational status fail to differentiate the two inhibitors but it also did not predict overall

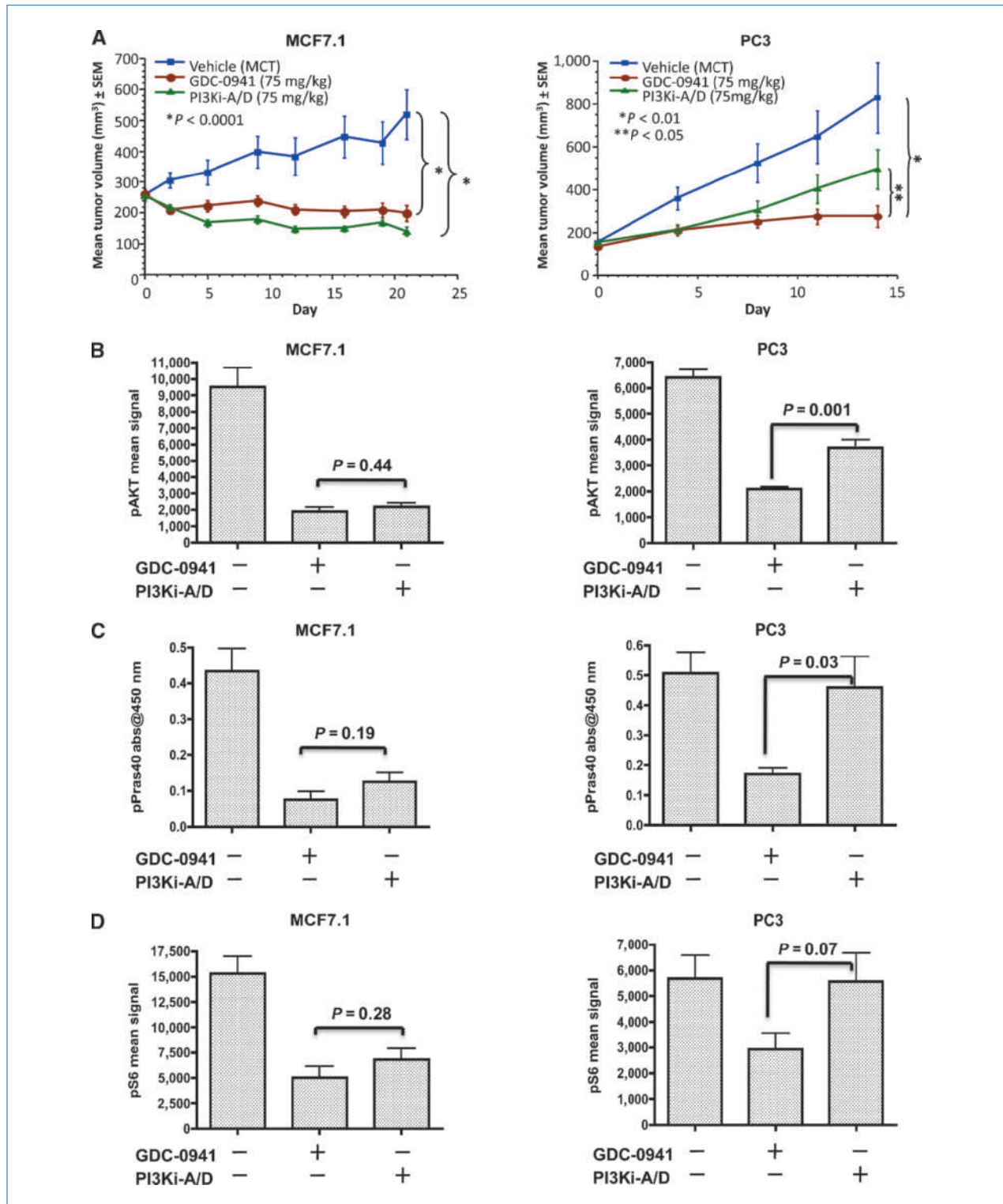


**Figure 5.** *In vivo* pathway effects of GDC-0941 and PI3Ki-A/D. A, MCF7.1 breast tumor and NCI-PC3 prostate cells were implanted s.c. in the hind flanks of female athymic nu/nu (nude) mice. Tumor-bearing mice were dosed orally with vehicle (0.5% methylcellulose/0.2% Tween-80), 75 mg/kg GDC-0941, or 75 mg/kg PI3Ki-A/D for 21 or 14 continuous days for MCF7.1 or NCI-PC3, respectively. \*, P values were determined by Student's *t* test. B–D, MCF7.1 or NCI-PC3 tumor-bearing mice were given a single dose of vehicle (MCT), 75 mg/kg PI3Ki-A/D, or 75 mg/kg GDC-0941 orally and tumors were harvested at 4 h post-dose. Tumor lysates were analyzed for pharmacodynamic changes by measuring pAkt (Ser<sup>473</sup>) (B), pPras40 (Thr<sup>246</sup>) (C), and pS6 (Ser<sup>235/236</sup>) (D). P values were determined by Student's *t* test.

**Table 2. Pharmacokinetic properties**

Species	Compound	CLp (mL/min/kg)	F%	Vss (L/kg)
Mouse	GDC-0941	64	78	2.8
	PI3Ki-A/D	29	56	1.5
Rat	GDC-0941	60	32	3.2
	PI3Ki-A/D	11	14	4.8

NOTE: Clearance (mL/min/kg), fraction of dose absorbed (F%), and volume of distribution (L/kg) in mouse and rat for GDC-0941 and PI3Ki-A/D.

sensitivity compared with those cell lines that were wild type for PIK3CA (Supplementary Fig. S3).

An increased role for p110 $\beta$  in PTEN-negative cancers and cell lines has been described recently (25–27). Jia and colleagues used a conditional knockout approach to study the tumorigenic and metabolic contributions of p110 $\beta$  in mice. Using a mouse prostate cancer model driven by PTEN loss, the authors showed that a coincident loss of p110 $\beta$  resulted in a striking decrease in prostate tumor formation, whereas tumor generation was not affected by the loss of p110 $\alpha$  in this model. Our results in cell lines and xenograft models with small-molecule inhibitors also support the importance of p110 $\beta$  inhibition in PTEN-negative tumors, although inhibition of both p110 $\alpha$  and p110 $\beta$  is needed to prevent tumor growth in PTEN-negative tumors. Taken together, p110 $\alpha$  may not be needed for tumor initiation in PTEN-negative tumors but seems to be required for tumor maintenance. Similar results were found using an inducible shRNA system to decrease the expression of class IA PI3K isoforms in PIK3CA-mutant and PTEN-deficient tumor cell lines (27). Consistent with previous data, PTEN-negative lines were strongly dependent on p110 $\beta$ . Surprisingly, in the same PTEN-negative lines, the authors showed that p110 $\alpha$  was not required for PI3K signaling or growth. These results differ from ours because we still observed efficacy in PTEN-negative tumors and cell lines without inhibiting p110 $\beta$ . In fact, we detected

significant pathway inhibition with PI3Ki-A/D in these lines at 4-hour treatments. The differences between these studies are likely due to the kinetics of compound inhibition in comparison with protein knockdown by shRNA or any potential noncatalytic effects of p110 isoforms. As expected, PIK3CA-mutant lines proved to be highly dependent on the p110 $\alpha$  isoform. A recent report describes a PTEN-associated complex that contains p110 $\beta$  (28). The PTEN-associated complex forms only when PTEN is not phosphorylated and has full enzymatic activity. Interestingly, the complex does not include p110 $\alpha$  and may suggest a possible mechanism for the increased role of p110 $\beta$  in PTEN-negative cancers.

Understanding the benefits and detriments of inhibitor specificities for cancer treatment is a key challenge in biomedical research. A major obstacle in this process is the availability of selective small-molecule tools. Here, we have used two closely matched small-molecule inhibitors of PI3K. The major difference between the two inhibitors is their potency against p110 $\beta$ . We show that the two inhibitors have similar activity in all tumors, except those lacking PTEN, wherein the additional inhibition of p110 $\beta$  results in increased potency. It is important to note, however, that the p110 $\alpha$ / $\delta$  inhibitor is still potent in PTEN-null cell lines and tumors. Understanding the molecular pathology of the tumor will be essential to matching patients with PI3K inhibitors of differing selectivity profiles.

#### Disclosure of Potential Conflicts of Interest

All authors are employees of Genentech, Inc.

#### Acknowledgments

We thank the Genentech PI3K chemistry team for the PI3K inhibitors; the Genentech bioanalytical scientists, Laurent Salphati, Jodie Pang, and Xiao Ding, for analysis of tumor drug concentrations; Cindy Hyung for cell culture support in all *in vivo* studies; and Peter Haverty for invaluable help and discussion.

The costs of publication of this article were defrayed in part by the payment of page charges. This article must therefore be hereby marked *advertisement* in accordance with 18 U.S.C. Section 1734 solely to indicate this fact.

Received 7/8/09; revised 11/12/09; accepted 12/4/09; published OnlineFirst 1/26/10.

#### References

- Campbell IG, Russell SE, Choong DY, et al. Mutation of the PIK3CA gene in ovarian and breast cancer. *Cancer Res* 2004;64:7678–81.
- Samuels Y, Wang Z, Bardelli A, et al. High frequency of mutations of the PIK3CA gene in human cancers. *Science* 2004;304:554.
- Bertelsen BI, Steine SJ, Sandvei R, Molven A, Laerum OD. Molecular analysis of the PI3K-AKT pathway in uterine cervical neoplasia: frequent PIK3CA amplification and AKT phosphorylation. *Int J Cancer* 2006;118:1877–83.
- Byun DS, Cho K, Ryu BK, et al. Frequent monoallelic deletion of PTEN and its reciprocal association with PIK3CA amplification in gastric carcinoma. *Int J Cancer* 2003;104:318–27.
- Barber DF, Alvarado-Kristensson M, Gonzalez-Garcia A, Pulido R, Carrera AC. PTEN regulation, a novel function for the p85 subunit of phosphoinositide 3-kinase. *Sci STKE* 2006;2006:e49.
- Actor B, Cobbers JM, Buschges R, et al. Comprehensive analysis of genomic alterations in gliosarcoma and its two tissue components. *Genes Chromosomes Cancer* 2002;34:416–27.
- van Dam PA, Vergote IB, Lowe DG, et al. Expression of c-erbB-2, c-myc, and c-ras oncoproteins, insulin-like growth factor receptor I, and epidermal growth factor receptor in ovarian carcinoma. *J Clin Pathol* 1994;47:914–9.
- Livasy CA, Reading FC, Moore DT, Boggess JF, Liningner RA. EGFR expression and HER2/neu overexpression/amplification in endometrial carcinosarcoma. *Gynecol Oncol* 2006;100:101–6.
- Cantley LC. The phosphoinositide 3-kinase pathway. *Science* 2002;296:1655–7.
- Bader AG, Kang S, Zhao L, Vogt PK. Oncogenic PI3K deregulates transcription and translation. *Nat Rev Cancer* 2005;5:921–9.
- Hawkins PT, Anderson KE, Davidson K, Stephens LR. Signaling through class I PI3Ks in mammalian cells. *Biochem Soc Trans* 2006;34:647–62.



12. Foukas LC, Claret M, Pearce W, et al. Critical role for the p110 $\alpha$  phosphoinositide-3-OH kinase in growth and metabolic regulation. *Nature* 2006;441:366–70.
13. Ciraolo E, Iezzi M, Marone R, et al. Phosphoinositide 3-kinase p110 $\beta$  activity: key role in metabolism and mammary gland cancer but not development. *Sci Signal* 2008;1:ra3.
14. Graupera M, Guillemet-Guibert J, Foukas LC, et al. Angiogenesis selectively requires the p110 $\alpha$  isoform of PI3K to control endothelial cell migration. *Nature* 2008;453:662–6.
15. Guillemet-Guibert J, Bjorklof K, Salpekar A, et al. The p110 $\beta$  isoform of phosphoinositide 3-kinase signals downstream of G protein-coupled receptors and is functionally redundant with p110 $\gamma$ . *Proc Natl Acad Sci U S A* 2008;105:8292–7.
16. Ghigo A, Hirsch E. Isoform selective phosphoinositide 3-kinase  $\gamma$  and  $\delta$  inhibitors and their therapeutic potential. *Recent Pat Inflamm Allergy Drug Discov* 2008;2:1–10.
17. Knight ZA, Gonzalez B, Feldman ME, et al. A pharmacological map of the PI3-K family defines a role for p110 $\alpha$  in insulin signaling. *Cell* 2006;125:733–47.
18. Vlahos CJ, Matter WF, Hui KY, Brown RF. A specific inhibitor of phosphatidylinositol 3-kinase, 2-(4-morpholinyl)-8-phenyl-4*H*-1-benzopyran-4-one (LY294002). *J Biol Chem* 1994;269:5241–8.
19. Davies SP, Reddy H, Caivano M, Cohen P. Specificity and mechanism of action of some commonly used protein kinase inhibitors. *Biochem J* 2000;351:95–105.
20. Yap TA, Garrett MD, Walton MI, Raynaud F, de Bono JS, Workman P. Targeting the PI3K-AKT-mTOR pathway: progress, pitfalls, and promises. *Curr Opin Pharmacol* 2008;8:393–412.
21. Jackson SP, Schoenwaelder SM, Goncalves I, et al. PI3-kinase p110 $\beta$ : a new target for antithrombotic therapy. *Nat Med* 2005;11:507–14.
22. Sadhu C, Dick K, Tino WT, Staunton DE. Selective role of PI3K $\delta$  in neutrophil inflammatory responses. *Biochem Biophys Res Commun* 2003;308:764–9.
23. Folkes AJ, Ahmadi K, Alderton WK, et al. The identification of 2-(1*H*-indazol-4-yl)-6-(4-methanesulfonyl-piperazin-1-ylmethyl)-4-morpholin-4-yl-thieno[3,2-*d*]pyrimidine (GDC-0941) as a potent, selective, orally bioavailable inhibitor of class I PI3 kinase for the treatment of cancer. *J Med Chem* 2008;51:5522–32.
24. Folkes A, inventor. Preparation of thienopyrimidines and furopyrimidines as lipid kinase inhibitors for treating cancer and other diseases. patent WO 2007127175. 2007.
25. Jia S, Liu Z, Zhang S, et al. Essential roles of PI(3)K-p110 $\beta$  in cell growth, metabolism and tumorigenesis. *Nature* 2008;454:776–9.
26. Torbett NE, Luna-Moran A, Knight ZA, et al. A chemical screen in diverse breast cancer cell lines reveals genetic enhancers and suppressors of sensitivity to PI3K isoform-selective inhibition. *Biochem J* 2008;415:97–110.
27. Wee S, Wiederschain D, Maira SM, et al. PTEN-deficient cancers depend on PIK3CB. *Proc Natl Acad Sci U S A* 2008;105:13057–62.
28. Rabinovsky R, Pochanard P, McNear C, et al. p85 associates with unphosphorylated PTEN and the PTEN-associated complex. *Mol Cell Biol* 2009;29:5377–88.

## Correction: Online Publication Dates for *Cancer Research* April 15, 2010 Articles

The following articles in the April 15, 2010 issue of *Cancer Research* were published with an online publication date of April 6, 2010 listed, but were actually published online on April 13, 2010:

Garmy-Susini B, Avraamides CJ, Schmid MC, Foubert P, Ellies LG, Barnes L, Feral C, Papayannopoulou T, Lowy A, Blair SL, Cheresh D, Ginsberg M, Varner JA. Integrin  $\alpha 4 \beta 1$  signaling is required for lymphangiogenesis and tumor metastasis. *Cancer Res* 2010;70:3042–51. Published OnlineFirst April 13, 2010. doi:10.1158/0008-5472.CAN-09-3761.

Vincent J, Mignot G, Chalmin F, Ladoire S, Bruchard M, Chevriaux A, Martin F, Apetoh L, Rébé C, Ghiringhelli F. 5-Fluorouracil selectively kills tumor-associated myeloid-derived suppressor cells resulting in enhanced T cell-dependent antitumor immunity. *Cancer Res* 2010;70:3052–61. Published OnlineFirst April 13, 2010. doi:10.1158/0008-5472.CAN-09-3690.

Nagasaka T, Rhees J, Kloor M, Gebert J, Naomoto Y, Boland CR, Goel A. Somatic hypermethylation of *MSH2* is a frequent event in Lynch syndrome colorectal cancers. *Cancer Res* 2010;70:3098–108. Published OnlineFirst April 13, 2010. doi:10.1158/0008-5472.CAN-09-3290.

He X, Ota T, Liu P, Su C, Chien J, Shridhar V. Downregulation of HtrA1 promotes resistance to anoikis and peritoneal dissemination of ovarian cancer cells. *Cancer Res* 2010;70:3109–18. Published OnlineFirst April 13, 2010. doi:10.1158/0008-5472.CAN-09-3557.

Fiorentino M, Judson G, Penney K, Flavin R, Stark J, Fiore C, Fall K, Martin N, Ma J, Sinnott J, Giovannucci E, Stampfer M, Sesso HD, Kantoff PW, Finn S, Loda M, Mucci L. Immunohistochemical expression of BRCA1 and lethal prostate cancer. *Cancer Res* 2010;70:3136–9. Published OnlineFirst April 13, 2010. doi:10.1158/0008-5472.CAN-09-4100.

Veronese A, Lupini L, Consiglio J, Visone R, Ferracin M, Fornari F, Zanasi N, Alder H, D'Elia G, Gramantieri L, Bolondi L, Lanza G, Querzoli P, Angioni A, Croce CM, Negrini M. Oncogenic role of *miR-483-3p* at the *IGF2/483* locus. *Cancer Res* 2010;70:3140–9. Published OnlineFirst April 13, 2010. doi:10.1158/0008-5472.CAN-09-4456.

Lu W, Zhang G, Zhang R, Flores LG II, Huang Q, Gelovani JG, Li C. Tumor site-specific silencing of *NF- $\kappa$ B p65* by targeted hollow gold nanosphere-mediated photothermal transfection. *Cancer Res* 2010;70:3177–88. Published OnlineFirst April 13, 2010. doi:10.1158/0008-5472.CAN-09-3379.

Geng H, Rademacher BL, Pittsenbarger J, Huang C-Y, Harvey CT, Lafortune MC, Myrthue A, Garzotto M, Nelson PS, Beer TM, Qian DZ. ID1 enhances docetaxel cytotoxicity in prostate cancer cells through inhibition of p21. *Cancer Res* 2010;70:3239–48. Published OnlineFirst April 13, 2010. doi:10.1158/0008-5472.CAN-09-3186.

Yoo BK, Chen D, Su Z-z, Gredler R, Yoo J, Shah K, Fisher PB, Sarkar D. Molecular mechanism of chemoresistance by astrocyte elevated gene-1. *Cancer Res* 2010;70:3249–58. Published OnlineFirst April 13, 2010. doi:10.1158/0008-5472.CAN-09-4009.

Lu ZH, Shvartsman MB, Lee AY, Shao JM, Murray MM, Kladney RD, Fan D, Krajewski S, Chiang GG, Mills GB, Arbeit JM. Mammalian target of rapamycin activator RHEB is frequently overexpressed in human carcinomas and is critical and sufficient for skin epithelial carcinogenesis. *Cancer Res* 2010;70:3287–98. Published OnlineFirst April 13, 2010. doi:10.1158/0008-5472.CAN-09-3467.

Hattermann K, Held-Feindt J, Lucius R, Mürköster SS, Penfold MET, Schall TJ, Mentlein R. The chemokine receptor CXCR7 is highly expressed in human glioma cells and mediates antiapoptotic effects. *Cancer Res* 2010;70:3299–308. Published OnlineFirst April 13, 2010. doi:10.1158/0008-5472.CAN-09-3642.

Nadiminty N, Lou W, Sun M, Chen J, Yue J, Kung H-J, Evans CP, Zhou Q, Gao AC. Aberrant activation of the androgen receptor by NF- $\kappa$ B2/p52 in prostate cancer cells. *Cancer Res* 2010;70:3309–19. Published OnlineFirst April 13, 2010. doi:10.1158/0008-5472.CAN-09-3703.

Acu ID, Liu T, Suino-Powell K, Mooney SM, D'Assoro AB, Rowland N, Muotri AR, Correa RG, Niu Y, Kumar R, Salisbury JL. Coordination of centrosome homeostasis and DNA repair is intact in MCF-7 and disrupted in MDA-MB 231 breast cancer cells. *Cancer Res* 2010;70:3320–8. Published OnlineFirst April 13, 2010. doi:10.1158/0008-5472.CAN-09-3800.

McFarlane C, Kelvin AA, de la Vega M, Govender U, Scott CJ, Burrows JF, Johnston JA. The deubiquitinating enzyme USP17 is highly expressed in tumor biopsies, is cell cycle regulated, and is required for G<sub>1</sub>-S progression. *Cancer Res* 2010;70:3329–39. Published OnlineFirst April 13, 2010. doi:10.1158/0008-5472.CAN-09-4152.

Dudka AA, Sweet SMM, Heath JK. Signal transducers and activators of transcription-3 binding to the fibroblast growth factor receptor is activated by receptor amplification. *Cancer Res* 2010;70:3391–401. Published OnlineFirst April 13, 2010. doi:10.1158/0008-5472.CAN-09-3033.

Cho SY, Xu M, Roboz J, Lu M, Mascarenhas J, Hoffman R. The effect of CXCL12 processing on CD34<sup>+</sup> cell migration in myeloproliferative neoplasms. *Cancer Res* 2010;70:3402–10. Published OnlineFirst April 13, 2010. doi:10.1158/0008-5472.CAN-09-3977.

---

Published OnlineFirst 05/11/2010.

©2010 American Association for Cancer Research.  
doi: 10.1158/0008-5472.CAN-10-1347

# Cancer Research

The Journal of Cancer Research (1916–1930) | The American Journal of Cancer (1931–1940)

## Isoform-Specific Phosphoinositide 3-Kinase Inhibitors Exert Distinct Effects in Solid Tumors

Kyle A. Edgar, Jeffrey J. Wallin, Megan Berry, et al.

*Cancer Res* 2010;70:1164-1172. Published OnlineFirst January 26, 2010.

<b>Updated version</b>	Access the most recent version of this article at: doi: <a href="https://doi.org/10.1158/0008-5472.CAN-09-2525">10.1158/0008-5472.CAN-09-2525</a>
<b>Supplementary Material</b>	Access the most recent supplemental material at: <a href="http://cancerres.aacrjournals.org/content/suppl/2010/01/26/0008-5472.CAN-09-2525.DC1">http://cancerres.aacrjournals.org/content/suppl/2010/01/26/0008-5472.CAN-09-2525.DC1</a>

<b>Cited articles</b>	This article cites 27 articles, 10 of which you can access for free at: <a href="http://cancerres.aacrjournals.org/content/70/3/1164.full#ref-list-1">http://cancerres.aacrjournals.org/content/70/3/1164.full#ref-list-1</a>
<b>Citing articles</b>	This article has been cited by 21 HighWire-hosted articles. Access the articles at: <a href="http://cancerres.aacrjournals.org/content/70/3/1164.full#related-urls">http://cancerres.aacrjournals.org/content/70/3/1164.full#related-urls</a>

<b>E-mail alerts</b>	<a href="#">Sign up to receive free email-alerts</a> related to this article or journal.
<b>Reprints and Subscriptions</b>	To order reprints of this article or to subscribe to the journal, contact the AACR Publications Department at <a href="mailto:pubs@aacr.org">pubs@aacr.org</a> .
<b>Permissions</b>	To request permission to re-use all or part of this article, contact the AACR Publications Department at <a href="mailto:permissions@aacr.org">permissions@aacr.org</a> .